Energy Technology

Supporting Information

A Crystalline/Amorphous Cobalt(II,III) Oxide Hybrid Electrocatalyst for Lithium–Air Batteries

S. Mohammad B. Khajehbashi,[a] Jiantao Li,[a] Manman Wang,[a] Lin Xu,[a, b] Kangning Zhao,[a] Qiulong Wei,[a] Changwei Shi,[a] Chunjuan Tang,[a] Lei Huang,[a] Zhaoyang Wang,[a] and Liqiang Mai*[a]

ente_201600381_sm_miscellaneous_information.pdf

Synthesis of pure cobalt nano-particles

All chemicals are chosen in analytical grade. At first 1.1896 g of $CoCl_2$.$6H_2O$ were dissolved into 35 ml of ethylene glycol under magnetic stirring till getting homogeneous red solution. Then 0.5 g of polyvinylpyrrolidone (PVP) was added very slowly to the above solution under strongly agitation. Subsequently, 10 ml of NaOH solution (5 M) of deionized water and 10 ml of ethylenediamine were added drop wise to the red solution with simultaneous strongly agitation under hood chamber condition. After one hour under strong agitation, the mixture was transferred into a 100 ml warm Teflon-lined autoclave, which was sealed tight and maintained at 200^{o}C for 24h. Then autoclave cool down to room temperature naturally and the precipitates were obtained by centrifugation. The precipitates were thoroughly rinsed with pure ethanol and deionized water 5 times and finally, residual materials dried at 70 ^{o}C for 24 h. [1]

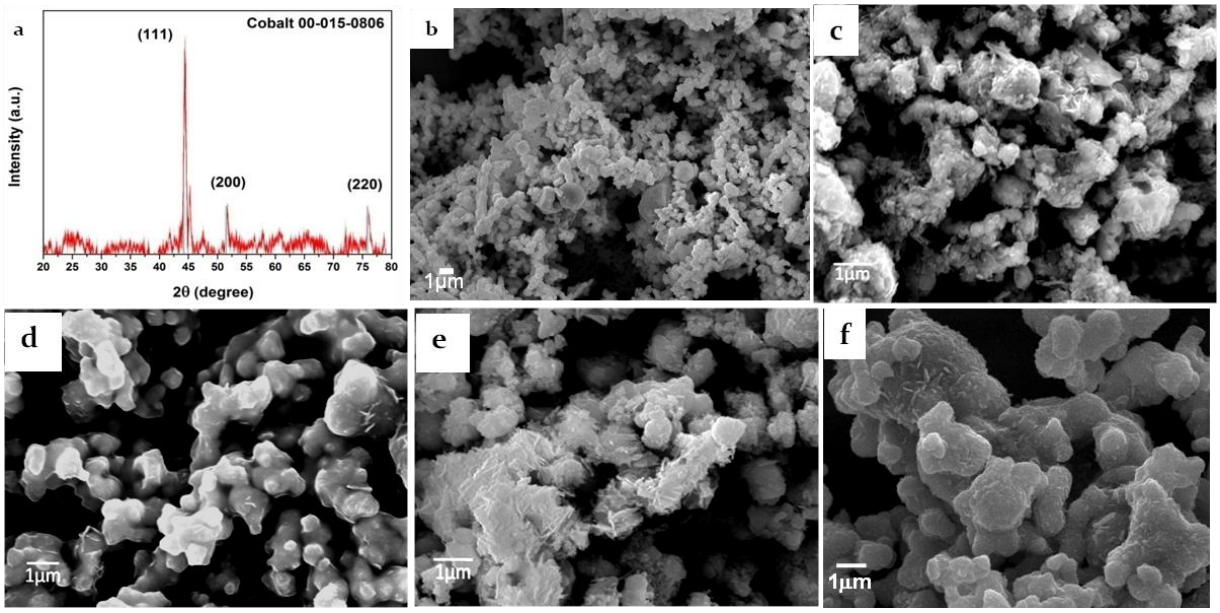

Figure S1. a) XRD pattern of Pure Co . SEM images of b) Pure Co, c) COX200, d) COX400, e) COX500 and f) COX650.

Rotating Disc Electrode (RDE) test and measurements

As mentioned in the main text the RDE test measurements is reliable method to study the kinetics of ORR. In brief to make the working electrode, catalyst and super P carbon (SPC) (3:7) dispersed in distilled water and isopropyl alcohol and sonicated for 2 hours then Na^+-exchanged Nafion solution added and again sonicated for 2h. Finally 8.5µl of prepared ink, drop casted to the pre-polished glassy carbon electrode (Pine Instruments), which gained a mass loading of 0.1 mg cm^{-2}. Working electrode vertically kept in covered container at room temperature to evaporate the solvent and then the working electrode was scanned at a rate of 5 mV s^{-1} while the rotating speed was set on 400, 625, 900, 1225, 1600 rpm respectively. After setting the speed in each step, the system was kept idle for several minutes to get the stable condition. As shown in Figure 2 and Figure S2, polarization curves for different speeds were obtained for COX200, COX400, COX500 and COX650. Koutecky-Levich plots (J^{-1} vs. $\omega^{-1/2}$) in the inset of Figure 2b were analyzed. After best linear fitting of the plots, the slope of the fitted lines put in the related equation and average of the results was reported as electron transfer number.

The koutecky-Levich equation for calculation of "n" is illustrated as below:

$$\frac{1}{J} = \frac{1}{J_L} + \frac{1}{J_K} = \frac{1}{B\omega^{1/2}} + \frac{1}{J_K}$$

$$B = 0.62nFC_0\,(D_0)^{2/3}\upsilon^{-1/6}$$

$$J_K = nFkC_0$$

Where J is the disc current density, J_K and J_L are the kinetic and diffusion-limiting current densities, ω is the angular velocity, n is transferred electron number, F is the Faraday constant (F=96485 C mol^{-1}), C_0 is the bulk concentration of O_2, D_0 is the diffusion coefficient of the electrolyte, υ is the kinematic viscosity of the electrolyte and k is the electron-transfer rate constant. In 0.1 M KOH solution, the value of mentioned constants are 1.2×10^{-6} mol cm^{-3}, 1.9×10^{-5} cm^2 s^{-1} and 0.01 cm^2 s^{-1} for C_o, D_0 and υ respectively.[2, 3]

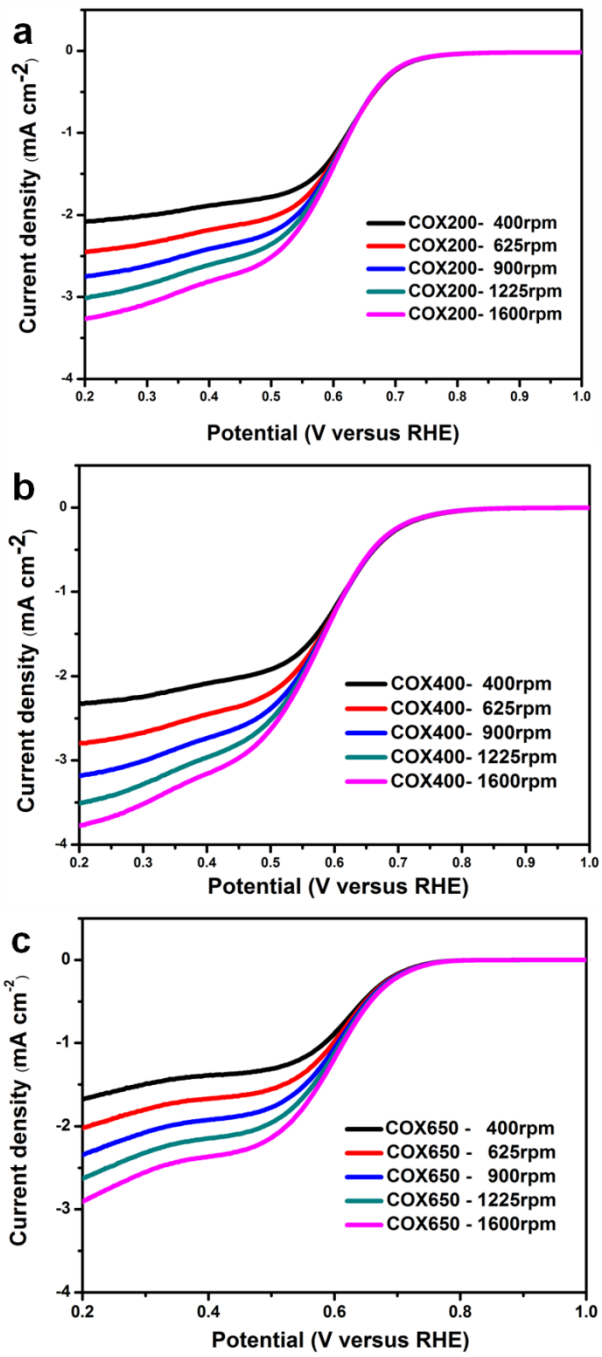

Figure S2. ORR polarization curves of a) COX200 (loading around 0.1 mg cm^{-2}), b) COX400 (loading around 0.1 mg cm^{-2}) in O_2-saturated 0.1M KOH and c) COX650 (loading around 0.1 mg cm^{-2}) in O_2-saturated 0.1M KOH.

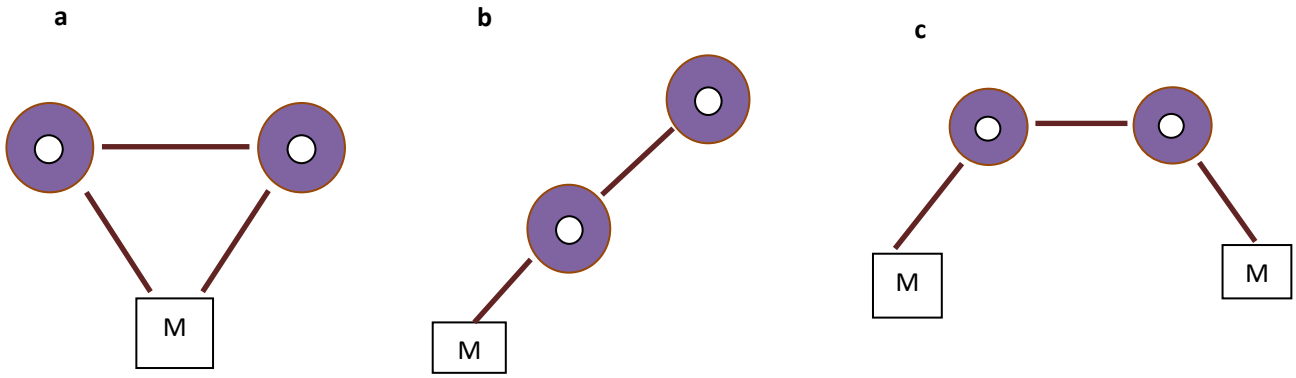

Figure S3. Oxygen adsorption models: (a) The Griffiths model, (b) The Pauling model, (c) The Yeager model. (O: oxygen atom, M: metal atom). (Ref.4)

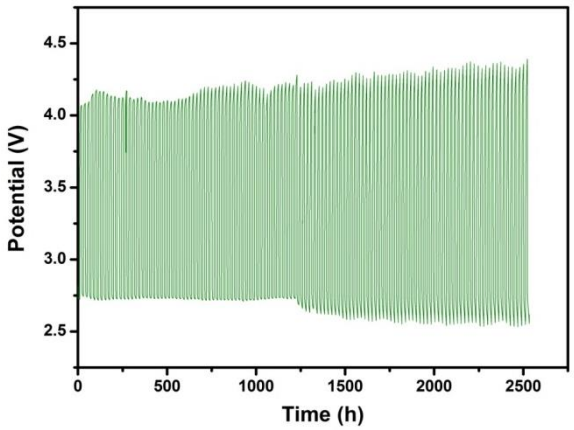

Figure S4. potential (V) versus real time of Li-air battery at a current density of 100 mA g^{-1}.

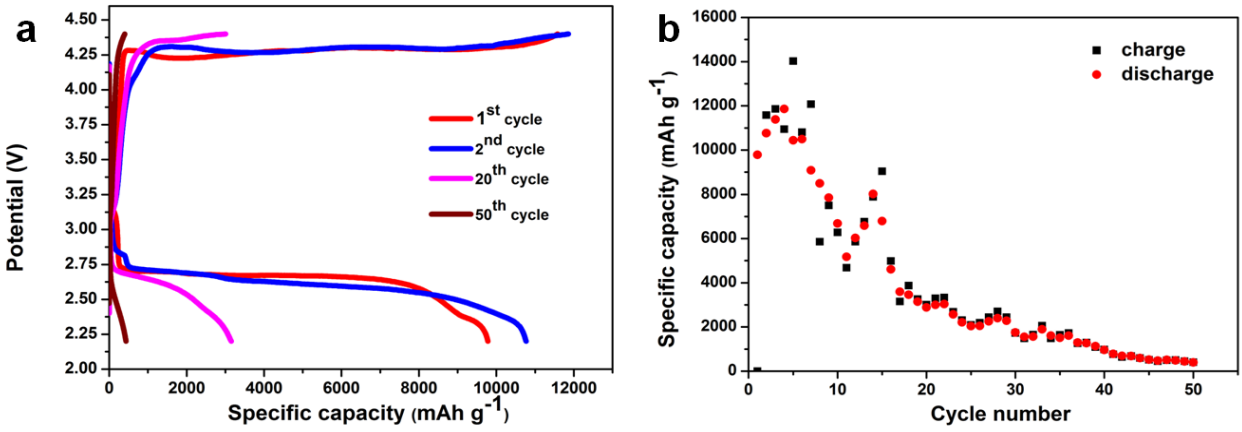

Figure S5. Fully charge/discharge test, a) specific capacity versus voltage at current density of 200 mA g^{-1} and b) cycling performance at current density of 200 mA g^{-1}.

Slow cooling sample

As found in the characterization results in the main text, the Raman spectroscopy in wide range can be a fast and reliable way to indicate the amorphous layer. The sample with 500 ^{o}C oxidation temperature and subsequent slow cooling in the furnace was characterized with Raman spectroscopy and then electrochemical performance was measured in assembled Li-air battery same as other samples. The Raman spectroscopy results and charge/discharge curves of Li-air battery with this catalyst are shown in Figure S6. Raman spectra in Figure S6 (a, b) show that the behavior of third sample with slow cooling condition is similar with COX400. As the base line is completely flat and there is no shoulder shape consists of Boson peaks, the lack of amorphous layer can be derived. Figure S6b shows in case of normal cooling the peaks are so compatible with references values.[5] Figure S6 (c, d) show the low performance of Li-air battery with this catalyst. The specific capacity in case of normal cooled sample could not reach the defined amount of 1000 mAh g^{-1}. Discharge potential decreased to around 2.6 V in first discharge and charging potential increased to around 4.4 V. Actually the capacity fading began from the beginning cycles. This low electrochemical performances beside the result of Raman spectra, confirm the key role of amorphous layer in hybrid catalyst. Amorphous layer beside the crystalline structure provide different active sites as mentioned in the mechanism section of main text.

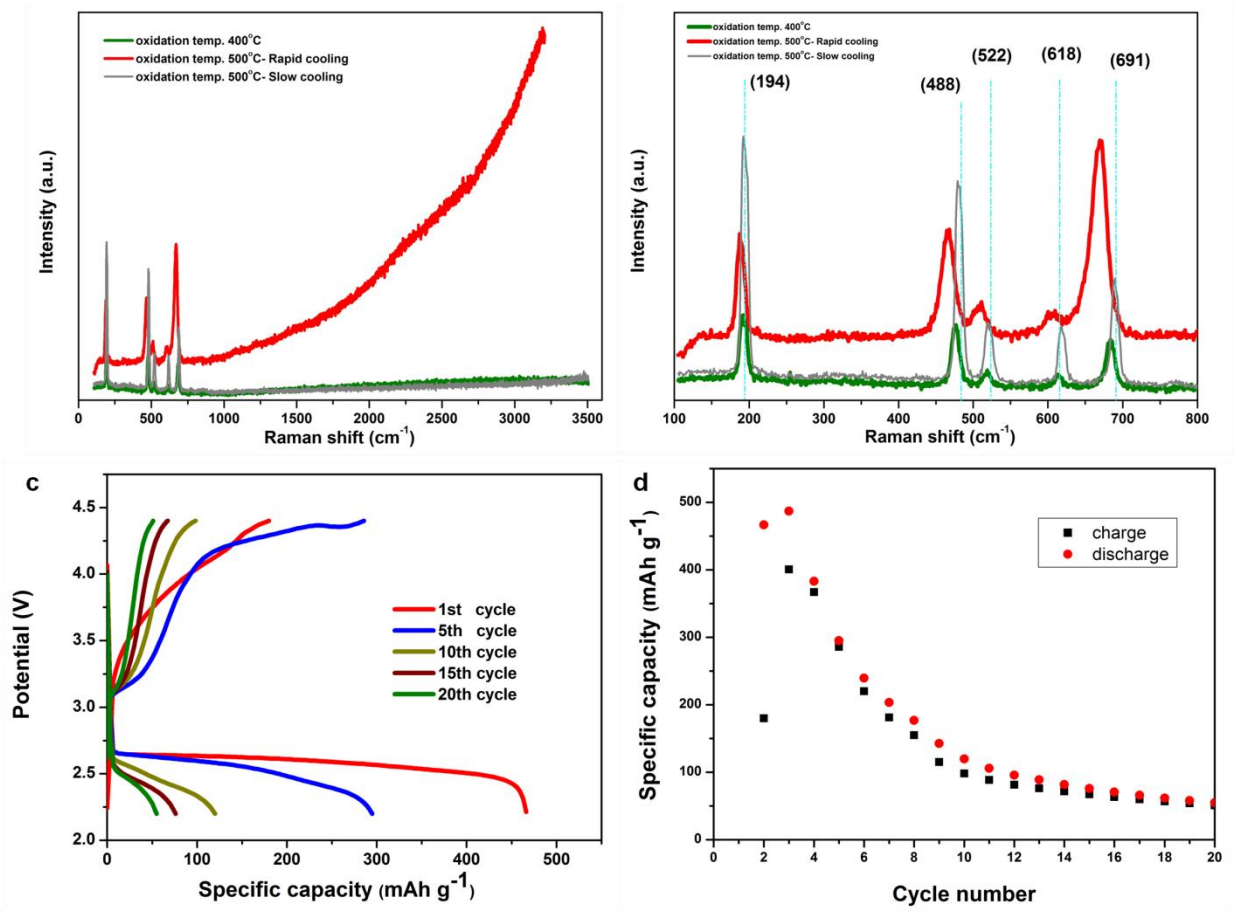

Figure S6. a, b) Raman spectra of COX400, COX500 and witness sample with oxidation at 500 ^{o}C and normal cooling in the furnace, c) Limited specific capacity (1000 mAh g^{-1}) versus voltage at current density of 100 mA g^{-1} for Li-air battery with slow (normal) cooled catalyst, d) cycling performance of Li-air battery with slow (normal) cooled catalyst.

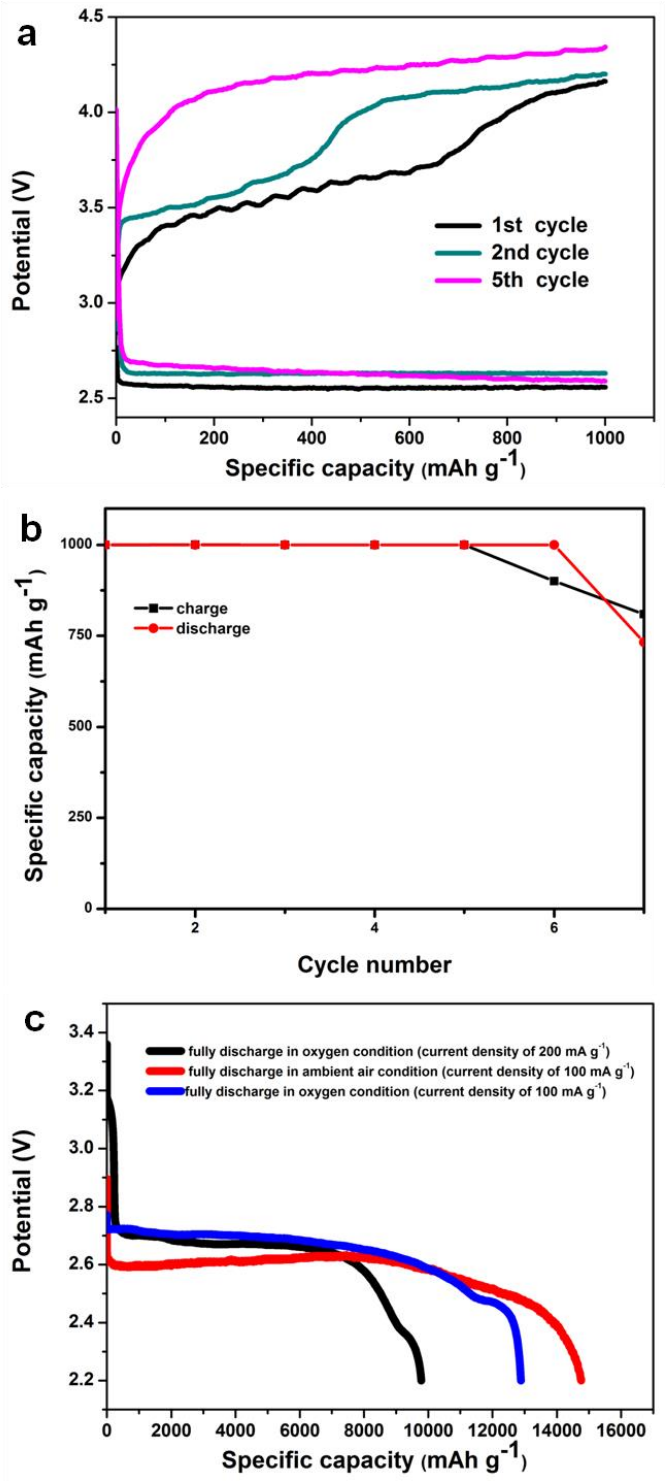

Figure S7. Li-air battery charge/discharge curves with COX500 catalyst in ambient air condition. a) Limited specific capacity (1000 mAh g^{-1}) versus voltage at current density of 200 mA g^{-1}, b) Cycle number versus limited specific capacity (1000 mAh g^{-1}) at current density of 200 mAg^{-1}, c) Comparison of first fully discharge in oxygen condition with ambient air condition.

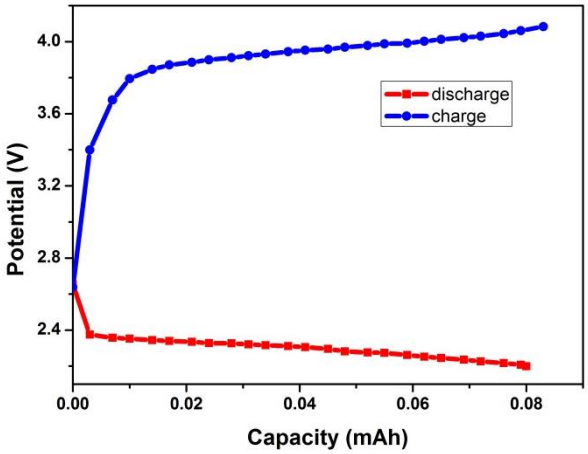

Figure S8. Charge/discharge curves of Li-air battery at current density of 200 mA g^{-1} during *in-situ* XRD testing.

Oxygen trapping calculations

According to the ideal gas law: PV= nRT

We consider the sphere shape for pores as Figure S9.

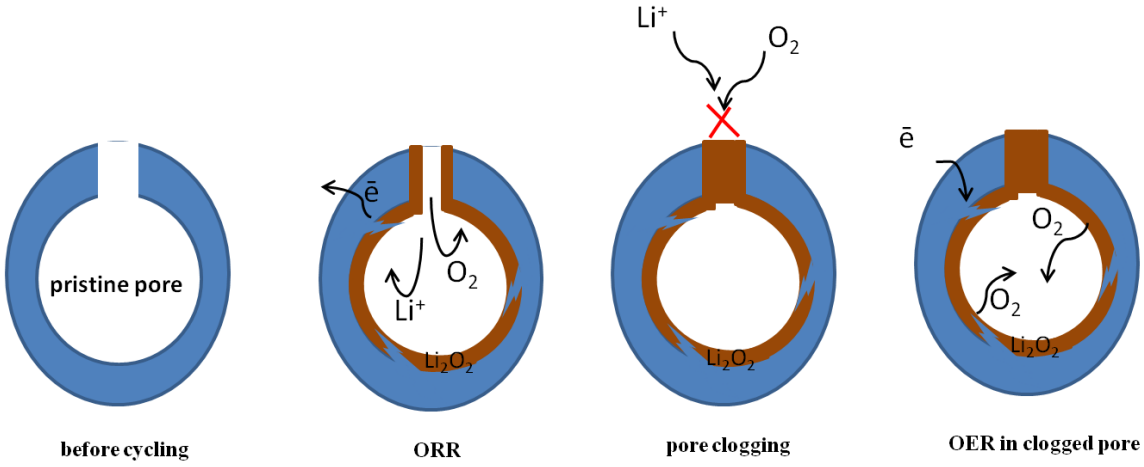

Figure S9. The Schematic illustration of pore blocking during the discharge and oxygen trapping during the charge in the blocked pore.

We have considered the pore size of catalyst around 1000 nm (as shown in Figure 1e, pore size is around 20 nm) and according to ideal gas law, smaller pore cause higher pressure so our estimation covers the actual pore size.

PV= nRT

For n = 1, T = 298 K and R = 0.0820 lit.atm.$mol^{-1}K^{-1}$

We consider pore diameter around 1000 nm. Then :

$V=5.2\times10^{-19}\ m^3$ $P=4.7\times10^{16}$ atm $\sim P = 4.7\times10^{21}$ Pa

$A=3.14\times10^{-12}\ m^2$ $F=1.5\times10^{10}\ N$

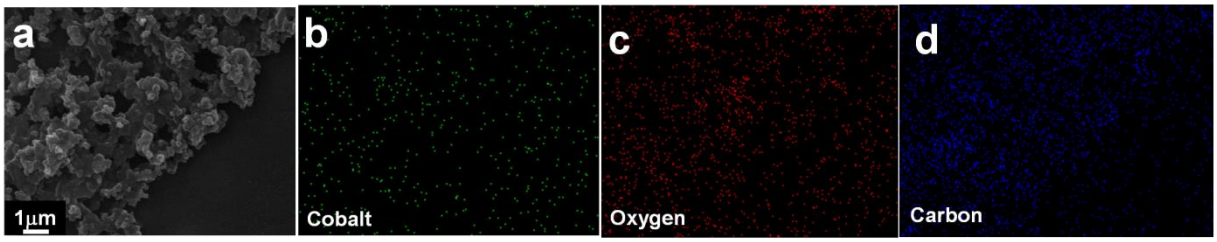

Figure S10. a) SEM image of cathode after charge. Energy dispersive X-ray spectroscopy (EDS) mapping of cathode after charge: b) cobalt, c) oxygen, d) carbon.

References

[1] X. Dong, M. Qi, Y. Tong and F. Ye, *Mater. Lett.* **2014**, 128, 39.
[2] Y. Liang, Y. Li, H. Wang, J. Zhou, J. Wang, T. Regier, H. Dai, *Nat. Mater.* **2011**, 10, 780.
[3] S. Mao, Z. Wen, T. Huang, Y. Hou, J. Chen, *Energy Environ. Sci.* **2014**, 7, 609.
[4] P. Sabatier, *Ber. Dtsch. Chem. Ges*. **1911**, 44, 1984.
[5] V. G. Hadjiev, M. N. Iliev, I. V. Vergilov, *J. Phys. C: Solid State Phys.* **1988**, 21, 199.